



HAL
open science

Strontium-82 and Future Germanium-68 Production at the ARRONAX Facility

Thomas Sounalet, Nathalie Michel, C. Alliot, A. Audouin, J. Barbet, A. C. Bonraisin, Y. Bortoli, V. Bossé, C. Bourdeau, G. Bouvet, et al.

► **To cite this version:**

Thomas Sounalet, Nathalie Michel, C. Alliot, A. Audouin, J. Barbet, et al.. Strontium-82 and Future Germanium-68 Production at the ARRONAX Facility. Nuclear Data Sheets, 2014, 119, pp.261-266. 10.1016/j.nds.2014.08.072 . hal-01206903

HAL Id: hal-01206903

<https://imt-atlantique.hal.science/hal-01206903v1>

Submitted on 19 Dec 2022

HAL is a multi-disciplinary open access archive for the deposit and dissemination of scientific research documents, whether they are published or not. The documents may come from teaching and research institutions in France or abroad, or from public or private research centers.

L'archive ouverte pluridisciplinaire **HAL**, est destinée au dépôt et à la diffusion de documents scientifiques de niveau recherche, publiés ou non, émanant des établissements d'enseignement et de recherche français ou étrangers, des laboratoires publics ou privés.

Strontium-82 and Future Germanium-68 Production at the ARRONAX Facility

T. Sounalet,¹ N. Michel,^{2,1} C. Alliot,^{2,3} A. Audouin,² J. Barbet,^{2,3} A.C. Bonraisin,²
Y. Bortoli,¹ V. Bossé,^{2,3} C. Bourdeau,² G. Bouvet,¹ J.M. Buhour,¹ A. Cadiou,¹ S. Fresneau,¹
M. Guillaumet,¹ F. Haddad,^{1,2,*} J. Laizé,² T. Millete,¹ F. Milon,² M. Mokili,^{1,2} and G. Montavon¹

¹*SUBATECH, Ecole des Mines de Nantes, Université de Nantes, CNRS/IN2P3,
4 rue Alfred Kastler, La Chantrerie, BP 20722, 44307 Nantes cedex 3 France*

²*GIP Arronax, 1 rue Aronnax, 44817 Saint-Herblain, France*

³*Département de Recherche en Cancérologie, Inserm, Université de Nantes,
U892, 8 quai Moncoussu, BP 70721, 44007 Nantes cedex 1, France*

The ARRONAX cyclotron is fully operational since the end of 2010. It delivers projectiles (p , d , α) at high energy (up to 70 MeV for protons) and high intensity ($2 \times 375 \mu A$ for protons). The main fields of application of ARRONAX are radionuclide production for nuclear medicine and irradiation of inert or living materials for radiolysis and radio-biology studies. A large part of the beam time will be used to produce radionuclides for targeted radionuclide therapy (copper-67, scandium-47 and astatine-211) as well as for PET imaging (scandium-44, copper-64, strontium-82 for rubidium-82 generators, and germanium-68 for gallium-68 generators). Since June 2012, large scale production of ^{82}Sr has started with rubidium chloride ($RbCl$) targets. Several improvements are being explored which consist of changing the target material from $RbCl$ to Rb metal and introducing an additional target behind the rubidium assembly. Thus, a target alloy of nickel/gallium for germanium-68 production has been developed. It is obtained by electroplating and exhibits a better thermal behavior than the natural gallium target used in most production facilities.

I. INTRODUCTION

ARRONAX (<http://www.cyclotron-nantes.fr/>) is a high energy and high intensity multi-particle cyclotron located in Nantes (France) which has been fully operational since the end of 2010. The facility is devoted to the production of radionuclides for medical applications and related topics as well as irradiation of inert or living materials for radiolysis and radio-biological studies. For radionuclide production, ARRONAX focuses on non-conventional radioisotopes [1]. Main applications cover oncology, cardiology and neurology. A priority list based on the capability of the machine as well as on the needs expressed by the nuclear medicine community has been created. This list contains radionuclides for both therapeutic use (^{67}Cu , ^{47}Sc and ^{211}At) and imaging ($^{82}Sr/^{82}Rb$ and $^{68}Ge/^{68}Ga$ generators and ^{64}Cu , ^{44}Sc). Routine production has started for ^{82}Sr whereas for ^{64}Cu , ^{211}At and ^{44}Sc , we are increasing the beam intensity on target in order to make these isotopes available for pre-clinical use. At the same time, we are setting up their production following good manufacturing practices (GMP) in order to use them in clinical trials in the near future.

Some work has also started on the production of ^{68}Ge which can be co-produced with ^{82}Sr . In section II, we describe our facility and its performance characteristics followed by a description of the production of ^{82}Sr in section III. Such a production has entered a routine mode since June 2012 and we will present the improvements that are foreseen in this production. Among them is the co-production of ^{68}Ge . The status on the targetry for that isotope production is presented in Section IV.

II. THE ARRONAX FACILITY

The heart of the ARRONAX Facility is a C70 cyclotron built by IBA, Belgium which can accelerate both positive ($HH+$, He^{++}) and negative ions (H^- , D^-) up to 70 MeV. Negative ions are extracted using the stripper foil technique. Particles at different energies can be extracted with a high efficiency (around 99%). For example, the proton beam can be extracted from 30 to 70 MeV. ARRONAX is equipped with two such diametrically-opposed devices giving the system the ability to extract two beams at the same time (dual beam mode). The machine has been built to deliver very intense beams ($375 \mu A$ for each proton beam).

Positive ions can be extracted using an electromagnetic

* Corresponding author: haddad@subatech.in2p3.fr

TABLE I. Main characteristics of the ARRONAX cyclotron.

Beam	Accelerated particles	Energy Range (MeV)	Intensity (μAe)	Dual mode
Protons	H-	30-70	≤ 375	yes
	HH+	17	≤ 50	no
Deuterons	D-	15-35	≤ 50	yes
	α	68	≤ 70	no

septum which is placed at a fixed position at the peripheral of the cyclotron. In this case, only one beam output is available at a fixed 68-MeV energy for alpha particles (extraction efficiency of the order of 83%). There is also the possibility to accelerate HH+ ions (extraction efficiency of 80%) at 34 MeV. This latter accelerated particle offers the possibility of having a proton beam at lower energy than that available using H- particles without the use of a beam energy degrader. The operational characteristics of ARRONAX are summarized in Table I. All these features have been validated during the commissioning phase of the machine. In particular, one of the tests consisted of delivering two proton beams at full intensity ($375 \mu\text{Ae}$) during 24h.

The cyclotron can deliver beams into six experimental vaults (see Fig. 1). Due to the extraction methods, proton and deuteron beams can be made available in all experimental vaults whereas α -particles and HH+ are only available in vaults A1, A2 and AX. Four halls, A1, A2, P2 and P3, are devoted to radionuclide production. They are equipped with a target station and a remote pneumatic transfer system (rabbit) to transfer irradiated materials from the beam lines to the hot cells. These two systems have been purchased from the cyclotron provider and modified to fulfill our requirements. These dedicated vaults allow flexibility and, together with the high intensity, will ensure the availability of radionuclides on a regular schedule. In addition, several laboratories for radiochemistry, biochemistry, hot cells, radio-labeling, chemical analysis, nuclear metrology are available.

A high-power accelerator-driven neutron source developed in collaboration with the Advanced Accelerator Application company (AAA) is installed in vault P1. This is part of the Theranean project [2] which aims at activation of injectable suspensions of nanoparticles carrying beta-emitting radioisotopes for brachytherapy. This project gathers interest in both academic laboratories and private companies. On the dedicated target developed within this project we have been able to use our cyclotron at full capacity.

The largest vault AX is our experimental area and is devoted to radiolysis, physics (cross section measurements and high energy PIXE) and radio-biology experiments. A beam entering this vault can be directed to three different sub-beam lines at the end of which the experimental devices are placed. One of the beam lines is directed to a pit providing a vertical beam. In this vault, the α -beam can be pulsed. Each pulse has a width equal to 3.3 ns and can contains up to $7 \cdot 10^6$ alphas. The delay

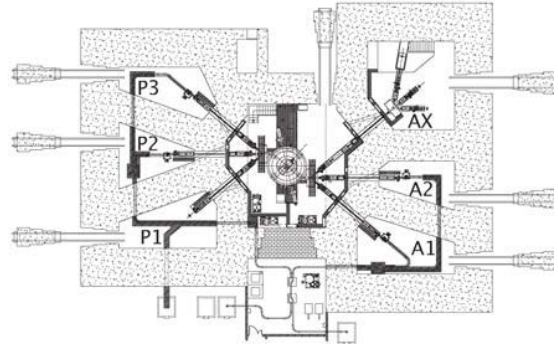


FIG. 1. Schematic view of the ARRONAX facility. This view does not show the different laboratories located around the vaults.

between consecutive pulses can vary from 330 ns up to a few seconds.

III. STRONTIUM-82 PRODUCTION

Among the different radioisotopes present in the priority list, ^{82}Sr ($T_{\frac{1}{2}}=25.34$ d) was the first one that came into large scale routine production at our facility. This radionuclide is the mother nucleus of the short lived rubidium-82 (^{82}Rb) isotope which is used in cardiology in the USA. This short lived radionuclide ($T_{\frac{1}{2}}=1.2575$ mn) is a β^+ emitter used to visualize poorly perfused myocardial zones resulting from coronary artery disease. As a β^+ emitter, it allows positron imaging tomography (PET imaging) and has shown superior diagnostic performances as compared to conventional single photon emission computer tomography (SPECT imaging) using either thallium-201 or technetium-99m for overweight patients or women [3]. ^{82}Rb has an ultra-short half-life which allows repeated injections to be made every 10 min and reduces the exposure of patients to radiation. Moreover, it is available through a generator which, with the good performance of the PET/Rb, makes rubidium very attractive. The $^{82}\text{Sr}/^{82}\text{Rb}$ generator is routinely marketed in the USA and there is a large and growing request from cardiologists worldwide. The most favorable route to produce ^{82}Sr is to use a proton induced reaction on a ^{nat}Rb target. In Fig. 2, the production cross section of this reaction is presented as a function of the incident proton energy. As one can see, this reaction has a high energy threshold above 30 MeV with a maximum of almost 100 mb around 50 MeV leading to an energy range of interest ranging from 40 MeV up to 70 MeV. The rather small value of the cross section indicates that large scale production must be conducted with a highly intense beam. These two facts, high energy and high intensity, explain why only a few places in the world are producing this radionuclide: Brookaven National Laboratory (BNL-USA), Los Alamos National Laboratory (LANL-USA),

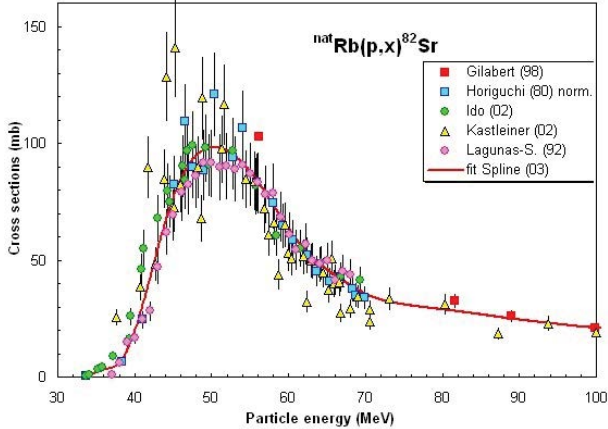


FIG. 2. Cross section of the reaction $^{nat}\text{Rb}(p,x)^{82}\text{Sr}$ as function of proton energy [4].

iThemba labs (South Africa), INR (Russia) and Triumf (Canada).

Since our facility possesses these two features, we have developed our own production of ^{82}Sr based on the use of rubidium chloride (RbCl) as the target material.

Approximately 4 g of RbCl (99.99% purity) pressed under 100 MPa are used to prepare the pellets. Each RbCl pellet (diameter 22 mm; thickness 4 mm) is then encapsulated in a compact laser welded stainless steel shell. Irradiation are performed using the irradiation station provided by IBA. To accommodate our RbCl targets in the irradiation station, we have developed our own rabbit keeping the external shape of the IBA design but changing totally the inside in order to get a high cooling capability with encapsulated targets. To optimize the production yield, we irradiate in dual target mode where two targets separated by a cooling gap of water are placed in a given rabbit. We also have decided to irradiate in the dual beam mode which means that two $100\mu\text{Ae}$ beams are extracted at the same time and sent onto two different irradiation stations. After irradiation, targets are processed using a Chelex-100 resin to extract and purify ^{82}Sr [5]. As compared to previous studies [6], it has been found that in our conditions, a Chelex-100 column is sufficient and no additional column is necessary. Using gamma-spectrometry for radioactive species and inductively coupled plasma optical emission spectrometry (ICP-OES) for stable elements, it has been proven that All specifications as in [7] are fulfilled with this process. Routine production have started in June 2012 using the dual beam mode with $100\mu\text{Ae}$ for each of the beam.

We are planning improvements to our set-up in order to optimize both the production yield and use of the proton beam. The first point consists to change the target material moving from RbCl to rubidium metal. By doing this, an increase by 30% of the production yield is expected. In addition, by using rubidium metal, the thermal conductivity of the target will be better, and an increase of the

beam current on target is also expected. However, there is a price to pay which is a much more complex handling of the target and of the chemical process. Indeed, as an alkaline, rubidium can highly react with water and air. A collaboration with the INR Troitsk (Russia), which uses Rb metal for many years, have been set for that purpose. The second development concerns the possibility to place another target behind the rubidium targets to get advantage of the outgoing protons. Indeed, most of the 70 MeV protons are passing through our targets without making nuclear interactions. They come out of our target arrangement with a kinetic energy around 40 MeV. At the moment, these protons are stopped in water in our targetry but it will be more interesting to use them to interact with a dedicated target to produce a useful radionuclide. A good candidate for this is germanium-68.

IV. GERMANIUM-68 PRODUCTION

Germanium-68 (^{68}Ge , $T_{1/2}=270.95$ d) is the parent nuclide of gallium-68 (^{68}Ga , $T_{1/2}=67.71$ min). The latter is a β^+ emitter used for PET imaging in oncology and can be obtained through a ^{68}Ge generator.

Germanium-68 can be produced using the $^{69}\text{Ga}(p,2n)^{68}\text{Ge}$ reaction. The cross section for this reaction is presented in Fig.3 as a function of the proton energy. The energy range of interest stretches from 30 MeV down to 15 MeV with a maximum value of 550 mb reached around 20 MeV. This energy range is in good agreement with the energy of our outgoing proton and the fact that a water gap must be put between the different targets to have a good cooling. The long half life of ^{68}Ge and moderate cross section require long irradiation times to achieve large production. This fact aligns with the coupling to strontium-82 production which stands for days.

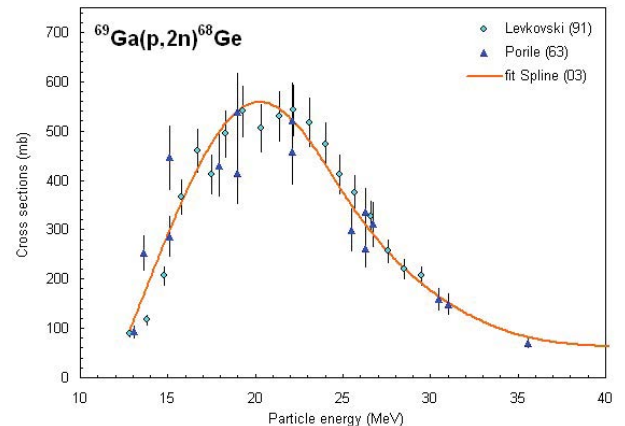


FIG. 3. Cross section of the reaction $^{69}\text{Ga}(p,2n)^{68}\text{Ge}$ as function of proton energy [4].

At the moment, most of the ^{68}Ge producers use natu-

ral gallium as a target material encapsulated in a niobium shell. However, this type of target is difficult to manage because of the properties of gallium: liquid at low temperature (around 30°C) and highly corrosive. During irradiation, corrosion problems and cracking are observed from time to time leading to the destruction of the target.

A solution to avoid this corrosion is to use an alloy metal which remains solid under irradiation conditions and contains a large portion of gallium. We have selected, as proposed by some authors [8], to work on a nickel/gallium alloy as target material.

The Ga-Ni phase diagram, Fig. 4, provides two kinds of information: the phases of the gallium /nickel alloy and their melting temperatures [9]. Ga_4Ni , Ga_3Ni_2 and Ga_4Ni_3 are three interesting phases with large mass proportions of gallium (between 60.8% and 80%). Their fusion temperatures are above 363°C. Simplified thermal calculations allow us to predict a surface temperature of our target below 230°C during irradiation which indicates that a target made of one of these alloys should stay solid during irradiation.

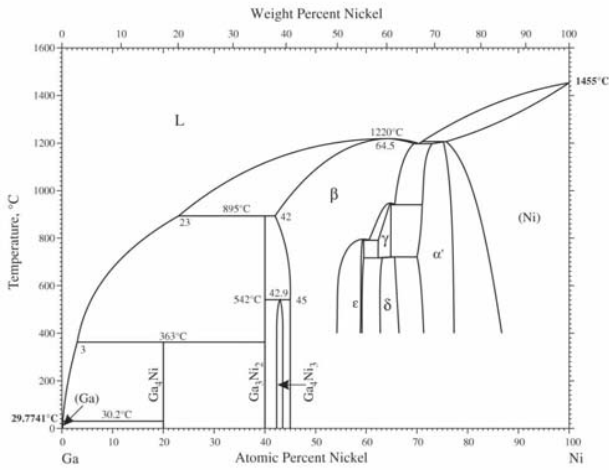


FIG. 4. Gallium-Nickel phase diagram.

We will now focus on the electroplating of the alloy, characterizations of the deposit and the expected ^{68}Ge yield with such targets. The electroplating solution contains Ni^{2+} and Ga^{3+} ions coming from $\text{Ga}_2(\text{SO}_4)_3$ and NiCl_2 . $\text{Ga}_2(\text{SO}_4)_3$ is prepared from gallium metal (Aldrich, 99.99% purity) dissolved in a mixed nitric and sulfuric acid solution in ultrapure water. The solution is evaporated to dryness to obtain gallium sulfate which is dissolved in dilute sulfuric acid (VWR, 95% purity) to pH 1.5 by heating at 50°C and stirring. Finally, to determine the exact gallium concentration, an ICP-OES analysis is done. Nickel ions are directly dissolved from nickel chloride (Alfa Aesar, 99.3% purity) in ultra-pure water. The two solutions are mixed and the pH is adjusted to 2 by means of NaOH addition. This electrolyte is transferred to a homemade electroplating cell made of Teflon. The surface of the deposit (3.24 cm²) is defined by the silicone

seal. The potentiostat used for electroplating was a radiometer PGP 201 from Metrohm. The cathode was the gold backing and the anode a platinum rod (99.95% purity, 5 mm diameter, 85 mm length, from Neyco, France). A gold backing has been chosen because of its good thermal conductivity and resistance to corrosion. Potentials were measured against an SCE reference electrode and the temperature was regulated. During electroplating the solution was stirred with a stirring magnetic rod.

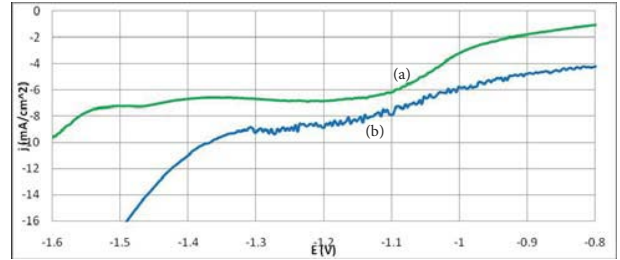


FIG. 5. Voltammetric response for the reduction of Ga^{3+} (curve a) and Ni^{2+} (curve b) at gold electrode with $[\text{Ga}^{3+}] = [\text{Ni}^{2+}] = 0.01 \text{ mol.L}^{-1}$ and pH=2.

The voltammetric technique was first used to gain information about the general behavior of the electroplating process. Figure 5 shows the potentiometric runs at pH=2 in 1M Cl^- in the presence of Ga^{3+} or Ni^{2+} . The deposition of gallium occurs at high overpotentials in acid chloride solution [10]. Two swallow changes are observed for gallium at -1.1 V/NHE and -1.45V/NHE. The first corresponds to a reduction of Ga^{3+} in Ga^+ . The second one is the one of interest and corresponds to the reduction of Ga^{3+} in gallium [11]. The nickel reduction is observed around -1.2V/NHE as we can observe a swallow modification at this value. Since Ga^{3+} needs higher potential value to be reduced, it is harder to reduce. Its deposition had to be promoted over nickel. So we have chosen a potential value at -1.6 V/NHE more favorable to gallium plating. At this voltage, hydrogen evolution which occurs simultaneously is not an issue.

Once the plating voltage has been chosen, different parameters were tested: concentration of gallium and nickel in solution, plating temperature, and stirring system. An alloy layer up to 300 μm thick over an area of 3.24 cm² has been successfully electroplated onto a gold backing using our device. The parameters used were: $[\text{Ga}^{3+}] = 0.5 \text{ M}$, $[\text{Ni}^{2+}] = 0.25 \text{ M}$, a solution temperature of 40°C, and a stirring speed of 1300 rpm. It takes six hours to obtain such a deposit.

The alloy deposit has been characterized by several methods. A stereo microscope LEICA M165C with 16.5:1 zoom, a scanning electron microscope (SEM, JEOL 5800LV) operated at 15 kV coupled to a quantitative energy dispersive X-ray (EDX) analyzer were used to examine the surface characteristics of the electroplated alloy. Sixteen measurements spread over the surface area were made. The micro-structure of the deposits was investigated by means of X-Ray diffraction (Siemens

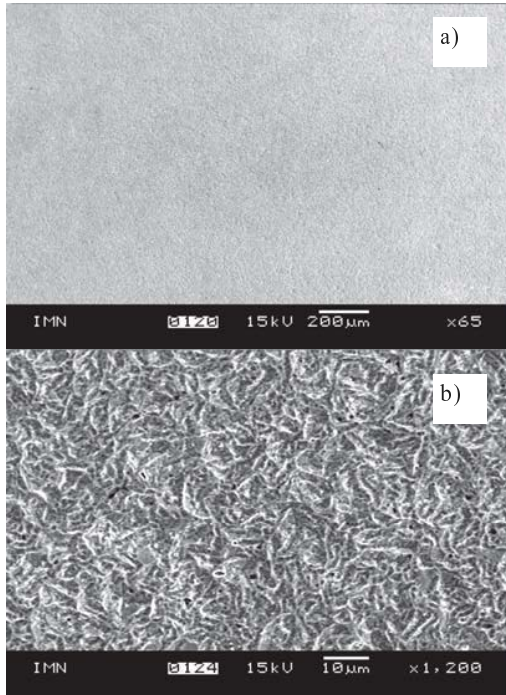


FIG. 6. SEM images with a magnification of 65 (a) and 1200 (b) of Ga-Ni alloy.

D5000). An ICP-OES Thermo Scientific iCAP Series 6500, equipped with a charge injection device (CID) detector CETAC and Asx-520 Autosampler (France), was used to determine the concentration of elements in the electrolyte and deposit.

A good target deposit for radionuclide production must be smooth, dense, stress free, and homogeneous [12]. Figure 6 shows SEM images of the Ga-Ni alloy obtained. The target layers are smooth (dendrite-free) and dense. There is no need for post mechanical preparation.

The composition of the deposit has been determined using EDX analyzer and ICP-OES to be only gallium and nickel. The deposit is free of traces of bath additives. We have followed the mass percentage of gallium in deposit at different plating times. This percentage remains stable with a value between 60% and 64% and an uncertainty of 5%, which may correspond to Ga_4Ni_3 phase.

We also performed XRD measurements to determine the structure of the Ni-Ga alloy (see Fig. 7). The XRD pattern of the electroplated Ga-Ni does not change during deposit and shows two main peaks at $2\theta=31.33^\circ$ and $2\theta=65.37^\circ$. These two positions correspond to X-ray diffraction on the (400) and (800) planes of Ga_4Ni_3 identified by the Miller indices. These peaks coming from pat-

tern of a Ga_4Ni_3 obtained by electroplating are stronger than for a pattern from a powder Ga_4Ni_3 specimen. All the others peaks that should be present are missing. This is due to the texture of the obtained solid. A peak that is stronger than all others peaks in a pattern relative to peaks from a random specimen identifies a direction of preferred crystallography orientation that is normal to the diffraction planes for the peaks [13]. In fact this pattern matches well with a Ga_4Ni_3 structure preferentially oriented along the axis [100] normal to (400) and (800) planes. It's a body-centered cubic structure.

This pattern matches well with a Ga_4Ni_3 structure preferentially oriented along the axis [400]. This layer remains intact after being heated up to 250°C in air but melts above 400°C . However, this behavior does not match with the properties of Ga_4Ni_3 derived from the phase diagram.

These analyses suggest that we have produced a phase close to Ga_4Ni_3 but additional studies, like thermogravimetric analysis and transmission electronic microscopy, need to be performed to define exactly the phase.

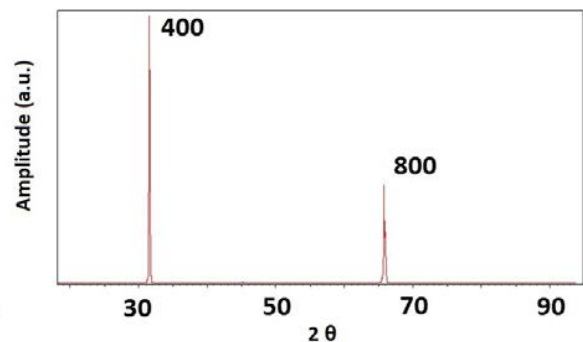


FIG. 7. XRD pattern obtained for Ga-Ni phase. Two main peaks are observed which correspond to the X-ray diffraction on the planes identified by the miller indices (400) and (800).

Assuming a Ga_4Ni_3 phase, we calculate that a 21-MeV proton beam with an intensity of $100 \mu\text{A}$ impinging on a $300 \mu\text{m}$ alloy target will produce 100 mCi of ^{68}Ge after 100 hours of irradiation. This calculation takes into account the shell material (niobium). Using the SRIM code [14], we found that the Bragg peak of the protons occurs beyond the target, in the cooling water. Under such conditions, thermal simulations indicate that the temperature in the target should stay below 300°C .

V. CONCLUSIONS

The ARRONAX cyclotron has been fully operational since the end of 2010, delivering different projectile types at high energy and high intensity. A priority list covering radioisotopes for both imaging and therapy has been defined. Large scale routine production of ^{82}Sr began in June 2012 using RbCl targets. Several improvements are foreseen: (a) changing the target material from RbCl

to Rb metal with the aim of achieving higher yields and better thermal conductivity to allow higher beam current on target; (b) introduction of an additional target to produce ^{68}Ge during the strontium-82 irradiation. We have developed a target made of Ni/Ga which has a higher melting point than natural gallium. Characterization of the phase obtained during electroplating is under study.

Initial thermal calculations indicate that germanium-68 production may be possible using this material as target.

Acknowledgments: The ARRONAX cyclotron is a project promoted by the Regional Council of Pays de la Loire financed by local authorities, the French government and the European Union. This work is partially financed by the OseO grant quanticardi (# F1110023).

- [1] F.Haddad *et al.*, EUR. J. MED. MOL. IMAGING **35**, 1377 (2008).
- [2] S. Buono *et al.*, PHYSICS FOR HEALTH IN EUROPE WORKSHOP (February 2-4, 2010, Geneva, Switzerland), http://www.adacap.com/files/files_dwl/00068.pdf.
- [3] D. Le Guludec *et al.*, EUR. J. NUCL. MED. MOL. IMAGING **35**, 1709 (2008).
- [4] IAEA-TECDOC 1211 (2001).
- [5] C. Alliot *et al.*, APPL. RADIAT. ISOT. **74**, 56 (2013).
- [6] L. Mausner, T. Prach, S. Srivastava, APPL. RADIAT. ISOT. **38**, 181 (1987).
- [7] D.R. Phillips *et al.*, RADIOCHIM. ACTA **88**, 149 (2000).
- [8] C. Loch, B. Maziere, D. Comar, R.Knipper, J. APPL. RADIAT. ISOT. **33**, 267 (1982).
- [9] H. Okamoto, J. PHASE EQUIL. **29**, 3 (2008).
- [10] D.O. Flamini, S.B. Saidman, J.B. Bessone, J. APPL. ELECTROCHEM. **37**, 467 (2007).
- [11] M. Ellner, K.J. Best, H. Jacobi, K. Schubert, J. LESS-COMMON METALS **19**, 294 (1969).
- [12] IAEA Technical report 432 (2004).
- [13] Crystallographic texture in ceramics and metals, Journal of Research of the National Institute of Standards and Technology, vol 206, number 6, November-December 2001.
- [14] J.F. Ziegler, J.P. Biersack, U. Littmark, The Stopping and Range of Ions in Solids, Pergamon Press, New York (1985).